



**HAL**  
open science

# Seasonal dynamics in microbial trace metals transporters during phytoplankton blooms in the Southern Ocean

Yanhui Kong, Rui Zhang, Stéphane Blain, Ingrid Obernosterer

## ► To cite this version:

Yanhui Kong, Rui Zhang, Stéphane Blain, Ingrid Obernosterer. Seasonal dynamics in microbial trace metals transporters during phytoplankton blooms in the Southern Ocean. *Environmental Microbiology*, 2024, 26 (10), 10.1111/1462-2920.16695 . hal-04748876

**HAL Id: hal-04748876**

**<https://hal.science/hal-04748876v1>**

Submitted on 22 Oct 2024

**HAL** is a multi-disciplinary open access archive for the deposit and dissemination of scientific research documents, whether they are published or not. The documents may come from teaching and research institutions in France or abroad, or from public or private research centers.

L'archive ouverte pluridisciplinaire **HAL**, est destinée au dépôt et à la diffusion de documents scientifiques de niveau recherche, publiés ou non, émanant des établissements d'enseignement et de recherche français ou étrangers, des laboratoires publics ou privés.

1       **Seasonal dynamics in microbial trace metals transporters during**  
2                   **phytoplankton blooms in the Southern Ocean**

3

4                   Yanhui Kong<sup>1,2</sup>, Rui Zhang<sup>2</sup>, Stéphane Blain<sup>2</sup>, Ingrid Obernosterer<sup>2\*</sup>

5

6   Affiliations

7    1 - School of Oceanography, Shanghai Jiao Tong University, 1954 Huashan Rd.,  
8    Shanghai 200030, China

9    2 - Sorbonne Université, CNRS, Laboratoire d'Océanographie Microbienne, LOMIC,  
10   Banyuls-sur-Mer, France

11

12   \* Correspondence to [ingrid.obernosterer@obs-banyuls.fr](mailto:ingrid.obernosterer@obs-banyuls.fr)

13

14

15       **Key words:** prokaryotic trace metals transporters; metagenomics; MAGs;

16   autonomous sampler; Southern Ocean;

17

18

19 **Abstract**

20

21 Trace metals are required as co-factors in metalloproteins that are essential in microbial  
22 metabolism and growth. The microbial requirements of diverse metals and the  
23 capabilities of prokaryotic taxa to acquire these metals remain poorly understood. We  
24 present here results from metagenomic observations over an entire productive season  
25 in the region off Kerguelen Island (Indian Sector of the Southern Ocean). We observed  
26 seasonal patterns in the abundance of prokaryotic transporters of 7 trace elements (Zn,  
27 Mn, Ni, Mo, W, Cu, Co) and the consecutive spring and summer phytoplankton blooms  
28 were strong drivers of these temporal trends. Taxonomic affiliation of the functional  
29 genes revealed that the transporters of these trace metals were associated to different  
30 microbial assemblages. Our observations suggest that *Rhodobacteraceae* had a broad  
31 repertoire of trace metal transporters (Mn, Zn, Ni, W, Mo) and a more restricted set was  
32 observed for other prokaryotic groups, such as *Flavobacteriaceae* (Zn), *Nitrincolaceae*  
33 (Ni, W) and *Thioglobaceae* (Mo). The prevalence of one or more trace metal  
34 transporters within a prokaryotic group, as determined on the family level, was overall  
35 confirmed in representative metagenome assembled genomes. We discuss the potential  
36 involvement of prokaryotic groups in processes related to organic matter utilization that  
37 require these metals and the consequences on carbon and trace metal cycling in surface  
38 waters of the Southern Ocean.

## 39 **Introduction**

40 The metals zinc (Zn), manganese (Mn), nickel (Ni), cobalt (Co), copper (Cu),  
41 molybdenum (Mo) and tungsten (W) are co-factors in metalloenzymes that drive the  
42 biogeochemical cycling of major elements. Diverse metal-containing enzymes are  
43 involved in the transformation and processing of dissolved organic matter (DOM), the  
44 major pool of organic carbon in the ocean. The utilization of different types of organic  
45 substrates within the DOM pool, covering a range of size fractions and varying degrees  
46 of bioavailability, is mediated by prokaryotes through pathways with distinct metal  
47 requirements. Zn is involved in carbohydrate-active enzymes (CAZymes) that play an  
48 important role in the degradation of polysaccharides (Hobbs et al. 2023), while Mn is  
49 required in the central carbon metabolism (Hansel 2017). Ni and Mo are both essential  
50 for nitrogen fixing microbes (Kuypers et al. 2018) and these elements are further  
51 involved in the utilization of nitrogen-containing substrates (Ni) and in carbon  
52 monoxide oxidation (Mo) (King and Weber, 2007). Methyloprobes require W for the  
53 utilization of substrates with no carbon-carbon bonds, including C1 compounds  
54 (Chistoserdova 2011). Cu, a catalyst in numerous cuproenzymes, has a major  
55 involvement in the respiratory enzyme cytochrome c oxidase in aerobic microbes  
56 (Ridge et al. 2008), and Co is mainly used as a key component of cobalamin (vitamin  
57 B12) synthesis (Bertrand et al. 2015). Despite the essential role of these elements in  
58 microbial metabolism and the cycling of DOM, little is known about the capacities of  
59 diverse prokaryotes to acquire these metals.

60

61 The key role of the trace element iron (Fe) for microbial communities in large parts of  
62 the ocean has motivated research on trace metal uptake mechanisms. The search for  
63 genes involved in the acquisition of different forms of Fe in individual genomes and  
64 metagenomes revealed that Fe<sup>3+</sup> transporters were common in marine prokaryotic  
65 genomes, while transporters for siderophore-bound Fe and heme were more abundant  
66 in *Gammaproteobacteria* and *Bacteroidetes* as compared to *Alphaproteobacteria*  
67 (Hopkinson and Barbeau, 2012). Exploring metagenome assembled genomes (MAGs)

68 from the Southern Ocean extended this view to taxonomy-specific differences in Fe-  
69 acquisition strategies (Sun et al. 2021). The use of distinct Fe-uptake mechanisms was  
70 further supported by metatranscriptomics approaches (Debeljak et al. 2019; Sun et al.  
71 2021). By contrast, the ecological strategies of prokaryotic taxa for the uptake of other  
72 essential trace metals has been less investigated. A genomic study revealed pronounced  
73 differences in the capacity of metal transport between *Roseobacter* and SAR11 (Hogle  
74 et al. 2016). While *Roseobacter* genomes contained transporters for several metals (Fe,  
75 Co, Ni, Cu, Zn), a reduced repertoire was present in SAR11 genomes (Hogle et al.  
76 2016). The potential role of *Rhodobacteraceae* in trace metal cycling was confirmed  
77 by gene expression patterns in experimental incubations (Debeljak et al. 2021).  
78 *Rhodobacteraceae* were major contributors to the transcripts of genes associated to the  
79 transport, sensing and regulation of nine metals (Zn, Mn, Cu, Co, Ni, Cd, Mo, W, and  
80 Fe) in Southern Ocean microbial communities (Debeljak et al. 2021). The diverse  
81 metabolisms present in marine microbial communities are likely strong drivers of the  
82 acquisition strategies of prokaryotic taxa, which in turn has implications on their role  
83 in the cycling of these elements in the ocean.

84 The main objectives of the present study were to identify genes encoding for the  
85 transport of seven metals (Zn, Mn, Ni, Mo, W, Cu, Co) in Southern Ocean prokaryotic  
86 communities, to investigate their temporal patterns over an entire productive season  
87 and to identify the key microbial players for each metal considered. We therefore  
88 searched for the respective genes in metagenomes obtained from microbial  
89 communities collected with an autonomous sampler in surface waters of the Central  
90 Kerguelen Plateau. Our observations are discussed with respect to a previous study in  
91 which we investigated the seasonal dynamics of Fe and organic substrate acquisition  
92 gene repertoires (Zhang et al. 2023).

93

94

## 95 **Experimental procedures**

### 96 Sample collection, DNA extraction and metagenome sequencing

97 We used 12 metagenomes obtained from seawater samples collected by the Remote  
98 Access Sampler (RAS) in surface waters (40 m) above the Kerguelen plateau (Station  
99 A3) in the Indian sector of the Southern Ocean (Blain et al. 2021). The details of DNA  
100 extraction and metagenome sequencing are given in the study by Liu et al. (2020) and  
101 Zhang et al. (2023). The data sets are available in the European Nucleotide Archive  
102 (ENA) repository at <https://www.ebi.ac.uk/ena> under the project ID PRJEB56376.

103

### 104 Metagenome assembly

105 Quality control (QC) passed reads from each sample were individually assembled by  
106 MEGAHIT v1.2.9 with default settings and metaSPAdes v3.15.2 (Nurk et al. 2017,  
107 parameters used -k 21, 33, 55, 77, 99, 127). After comparing the length of N50 produced  
108 by two tools (N50-MEGAHIT=690 bp, N50-metaSPAdes=935 bp), we finally used the  
109 metaSPAdes assembly results for analysis.

110

### 111 Metagenomic functional analysis

112 Open reading frames (ORFs) were predicted using Prodigal v2.6.3 (Hyatt et al. 2010,  
113 parameters used -p meta). CD-HIT v4.8.1 (Li & Godzik, 2006, parameters used -c 1 -  
114 aS 1 -g 1) was used to construct a non-redundant protein database. A total of 8.9 Mio  
115 non-redundant protein-coding genes were identified for all samples. Genes per kilobase  
116 million (GPM) were used as a proxy for gene abundance as described in Zhang et al.  
117 (2023). In order to identify the transporter sequences resulting from the individual  
118 metagenomic assemblies, predicted protein sequences were aligned using eggNOG 5.0  
119 (Huerta-Cepas et al. 2019) and GhostKOALA (Kanehisa et al. 2016) with default  
120 parameters. All KEGG orthologous (KO) numbers defined as “Transporter” in KEGG  
121 were retrieved, and metal transport-related genes were verified by reviewing previous  
122 literature and manually checking the metal transport information in the KEGG database

123 (Table S1). We then focused on genes related to the transport of trace metals into the  
124 cell, except for Co and Cu (see below). We used the *sitABCD* complex (Mn/Fe; Table  
125 S1) to refer to Mn transporters (Papp-Wallace & Maguire, 2006), as other Mn  
126 transporter proteins (e.g. *mnt*, *tro*) had low abundances or were undetectable in our  
127 sequences. Zn-transporters were identified based on ZIP2 (Grass et al. 2005) and  
128 *znuABC* (Hantke et al. 2001). While the ZIP family is known to contain several general  
129 trace metal transporters, the ZIP2 we used has been characterised as being specific for  
130 Zn (Grass et al. 2005). *Cbik* was used to refer to Ni transporters (Rodionov et al. 2006).  
131 Mo-transporters were identified based on *modABC* (Grunden & Shanmugam, 1997)  
132 and W-transporters were identified based on *tupAB* (Hagen, 2023). Genes for Co uptake  
133 were low and no Cu uptake genes were detected in our metagenomes, we therefore only  
134 considered the efflux systems of both metals and present the seasonal patterns for  
135 *cusABC* (for Cu) and *cnrABC*, *czcD* (for Co) (Franke et al. 2003; Okamoto & Eltis,  
136 2011).

137

138 Metagenomic taxonomic analysis and MAGs analysis

139 Taxonomic classification of metal-related genes was performed according to the  
140 Genome Taxonomy Database (Parks et al. 2022) using Centrifuge v1.0.4 (Kim et al.  
141 2016) and the alignments with highest score were kept. We mainly considered the  
142 family level and used metagenome-assembled genomes (MAGs) for a more fully  
143 resolved description. One MAG assigned to *Flavobacterium*, *Nitrincolaceae*,  
144 *Porticoccaceae*, SAR11, *Sphingomonadaceae* and *Thioglobaceae*, and two MAGs  
145 assigned to *Polaribacter* as well as four MAGs assigned to *Rhodobacteraceae* were  
146 downloaded from data previously published by Sun et al. (2021). Following the method  
147 described in the analysis of MAGs by Zhang et al. (2023), functional annotations of  
148 MAGs were performed and the abundances of MAGs and their metal transport-related  
149 genes across the 12 metagenomes were calculated. The coverage of the MAGs in each  
150 metagenome sample was determined by aligning reads from each sample back to the  
151 MAGs using Bowtie2 (Langmead & Salzberg, 2012). The mean coverage for each

152 MAG was then calculated from these alignments using anvio v7.1. This mean  
153 represents the average depth of coverage across contig, calculated as the coverage of  
154 each nucleotide in a contig divided by the length of the contig. Visualization of data  
155 was performed using the packages ggplot2 in the R v4.2.1 and SigmaPlot v14.5  
156 software.  
157



158 **Results**

159 Environmental context

160 The remote autonomous sampler (RAS) was deployed at station A3, located above the  
161 Kerguelen plateau southeast of Kerguelen Island (50.63°S, 72.06°E; overall depth  
162 527 m) in the Indian Sector of the Southern Ocean (Fig. 1). Samples were collected at  
163 40 m depth from 25 October 2016 to 24 February 2017 covering the entire productive  
164 season. During this time period temperature increased steadily from 4°C in early spring  
165 to 6° late summer (Fig. S1). The high concentrations of silicic acid at the beginning of  
166 the season (20  $\mu\text{M}$ ) rapidly decreased during spring (to 5  $\mu\text{M}$ ), while concentrations of  
167 nitrate remained elevated over the course of the season (20 to 30  $\mu\text{M}$ ) (Blain et al. 2021)  
168 (Fig. S1). Two consecutive phytoplankton blooms occurred during the sampling period,  
169 a spring bloom with a peak in mid-November and a summer bloom in early January  
170 (Fig. 1). Diatoms were the main contributors to phytoplankton biomass and revealed  
171 pronounced successional changes in community composition (Blain et al. 2021).  
172 Seasonal dynamics in prokaryotic community composition were strongly related to  
173 phytoplankton biomass and composition (Liu et al. 2020).

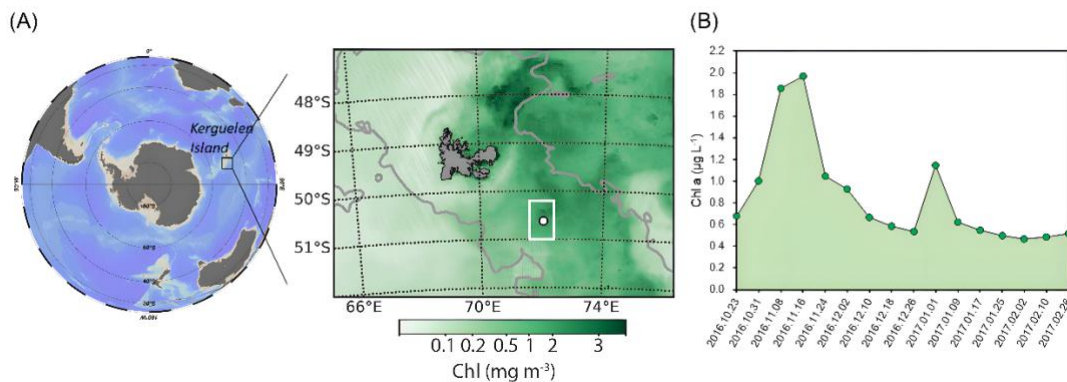


Figure 1. (A) Regional view of the mooring site on the Central Kerguelen plateau. The white dot denotes the position of the RAS mooring overlaying monthly chlorophyll for November 2016. Grey lines are the 1000 m isobaths. (B) Temporal changes of Chlorophyll *a* (green shaded area) during the period of the RAS deployment. Modified from Blain et al. (2021) and Liu et al. (2020).

175 Seasonal dynamics in trace element transporters

176 In a previous study we determined the temporal patterns of genes related to the uptake  
177 of different forms of iron (Fe) and of genes involved in the cleavage and uptake of  
178 organic substrates (Zhang et al. 2023). We focus here on genes related to the transport  
179 of the metals Mn, Zn, Ni, Mo, W, Co and Cu. A total of 89 metal transport related  
180 KEGG orthologous (KO) genes were retrieved from the KEGG database. Among these,  
181 67 KO genes were detected in our dataset and their normalized abundances varied  
182 between 0.2 to 760 genes per kilobase million (GPM) (Table S1, Fig. S2). We set a  
183 threshold for the further analyses with the aim to consider only the most abundant genes.  
184 We therefore considered only those KO genes for which the sum of the respective GPM  
185 in the 12 metagenomes was  $> 45$  GPM; this resulted in 26 KO genes (Table S1). The  
186 majority (84 %) of these transporters are metal uptake genes, and we also detected  
187 several efflux genes. In the case of Co, uptake genes had low abundance ( $< 40$  GPM)  
188 in our metagenomes, and no Cu uptake genes were detected.

189 Seasonal patterns of *sitABCD* (Mn/Fe transporters) revealed a sharp increase in GPM  
190 during the spring bloom and remained high until the summer bloom, followed by a  
191 rapid decline and a second smaller peak after the summer bloom (Fig. 2A). Transporters  
192 of Zn (*znuABC* and *ZIP2*), Ni (*cbiK*) and W (*tupAB*) increased after the spring bloom  
193 and their temporal patterns matched those of Mn over the remaining season (Fig. 2B,  
194 C, D). By contrast, transporters of Mo (*modABC*) had low GPM during the spring  
195 period, and revealed a small increase prior to and a marked peak after the summer  
196 bloom (Fig. 2E). As for Cu and Co, their efflux genes (*cusABC* for Cu and *cnrABC*,  
197 *czcD* for Co) had seasonally high GPM prior to and after the spring and summer blooms  
198 (Fig. 2F).

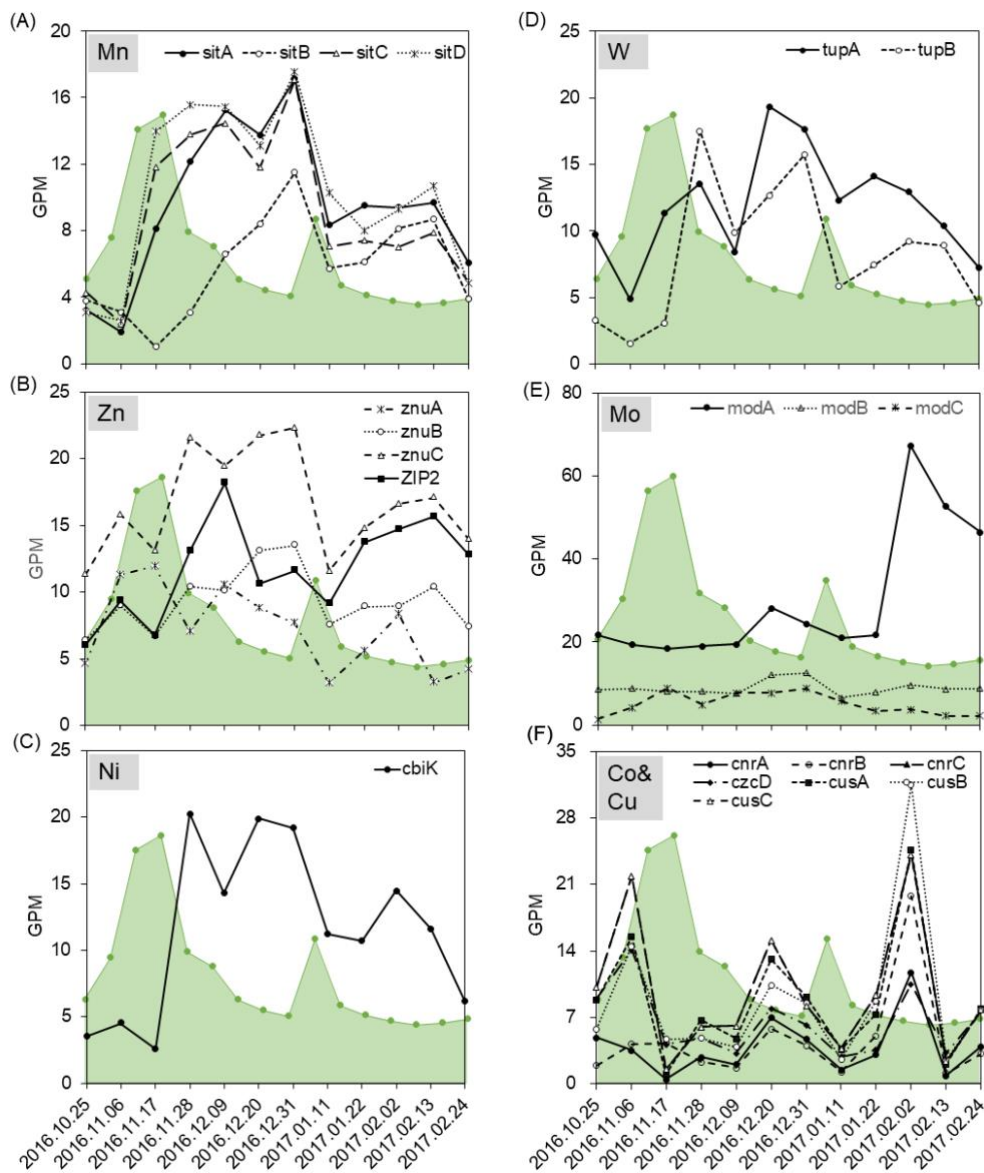


Figure 2. Temporal changes of Chlorophyll a (green shaded area) and abundance of genes for Mn transporters (A), Zn transporters (B), Ni transporters (C), W transporters (D), Mo transporters (E), and Co and Cu efflux transporters (F). Normalized gene abundances are given in genes per kilobase million (GPM).

199

200 Taxonomic affiliation of transporter genes

201 The taxonomic affiliations revealed pronounced differences in the relative contribution  
 202 of prokaryotic groups, at the family level, to the transporters of different trace metals  
 203 (Fig. 3). *Porticoccaceae* were the dominant contributors to *sitABCD* (Mn/Fe) during

204 the peak of the spring bloom and its early declining phase and *Rhodobacteraceae* had  
 205 an equal share during the remaining season. In the case of Zn, a contrasting picture was  
 206 obtained for the two types of transporters identified in our metagenomes. ZIP2 were  
 207 predominantly attributed to *Flavobacteriaceae*, with the exception of the start of the  
 208 spring bloom when *Pseudomonadaceae* had high contributions to ZIP2 transporters.  
 209 By contrast, taxonomic affiliations were more diverse for *znuABC* with seasonally  
 210 changing contributions of *Pseudomonadaceae*, *Porticoccaceae*, *Rhodobacteraceae* and  
 211 *Pelagibacteraceae*. The taxonomic assignments of *cbiK* (Ni) were dominated by  
 212 *Nitrincolaceae* after the spring bloom and *Rhodobacteraceae* and *Pelagibacteraceae*  
 213 were dominant contributors during the remaining season. Taxonomic assignments of  
 214 *tupAB* (W) were similar to those of *cbiK*. Transporters of Mo (*modABC*) were affiliated  
 215 to *Thioglobaceae*, *Pseudomonadaceae*, *Porticoccaceae*, and *Rhodobacteraceae*  
 216 throughout the season. *Pseudomonadaceae* and *Sphingomonadaceae* had similar  
 217 contributions to Co and Cu efflux transporters (Fig. S3).



Figure 3. Relative contribution of prokaryotic groups to specific genes associated with Mn (*sitABCD*), Zn (ZIP2 and *znuABC*), Ni (*cbiK*), W (*tupAB*) and Mo (*modABC*) transporters. Prokaryotic groups are based on the family level. Red arrows

indicate the spring phytoplankton bloom, and blue arrows indicate the summer phytoplankton bloom.

218

219 Metal acquisition genes in metagenome assembled genomes (MAG)

220 To identify the inventories of metal acquisition genes in individual prokaryotic taxa, we  
221 used previously published MAGs obtained from samples collected in the Kerguelen  
222 region, including our study site at the time point of the RAS deployment (Sun et al.  
223 2021). We chose 12 MAGs belonging to *Flavobacteriaceae*, *Nitriocolaceae*,  
224 *Porticoccaceae*, *Rhodobacteraceae*, SAR11, *Sphingomonadaceae* and *Thioglobaceae*  
225 (Fig. 4). These MAGs were chosen because they belong to prokaryotic groups with a  
226 substantial contribution to the different gene categories (Fig. 3). Moreover, ASVs  
227 belonging to these prokaryotic groups were shown to be abundant and have distinct  
228 seasonal relative abundance patterns (Liu et al. 2020). For some abundant prokaryotic  
229 groups with contributions to the genes of interest, as for example *Pseudomonadaceae*,  
230 no MAGs were previously annotated (Sun et al. 2023). Our results indicate that the  
231 *Rhodobacteraceae* MAGs (MAG 20, 23, 52, 106) had the most diverse and abundant  
232 metal transport gene inventories, including transporters of Mn, Zn, Ni, W, Mo, and Co,  
233 while MAGs belonging to other families had a reduced set of transporter genes. Two of  
234 the *Rhodobacteraceae* MAGs (20 and 52) had relatively high read-based coverage  
235 during the late declining stage of the spring bloom, while MAG106 had a less  
236 pronounced seasonal pattern. We detected Zn transporters (*znuABC* and *ZIP2*) in two  
237 *Flavobacteriaceae* MAGs (*Flavobacterium* MAG16 and *Polaribacter* MAG88) that  
238 had both highest coverage after the spring bloom. In addition, *Flavobacteriaceae*  
239 MAG16 harbored genes for Cu and Co efflux transporters. *Nitriocolaceae* MAG115  
240 contained transporters for Zn (*znu*), Ni (*cbik*) and W (*tup*) and had the highest coverage  
241 of all MAGs considered here, peaking during the early spring bloom decline. A  
242 contrasting seasonal coverage was observed for SAR11 MAG133 for which the W  
243 transporter *tup* was detected. *Sphingomonadaceae* MAG116 and *Thioglobaceae*  
244 MAG136 harbored both the Ni transporters (*cbik*), and MAG116 also contained *mod*.

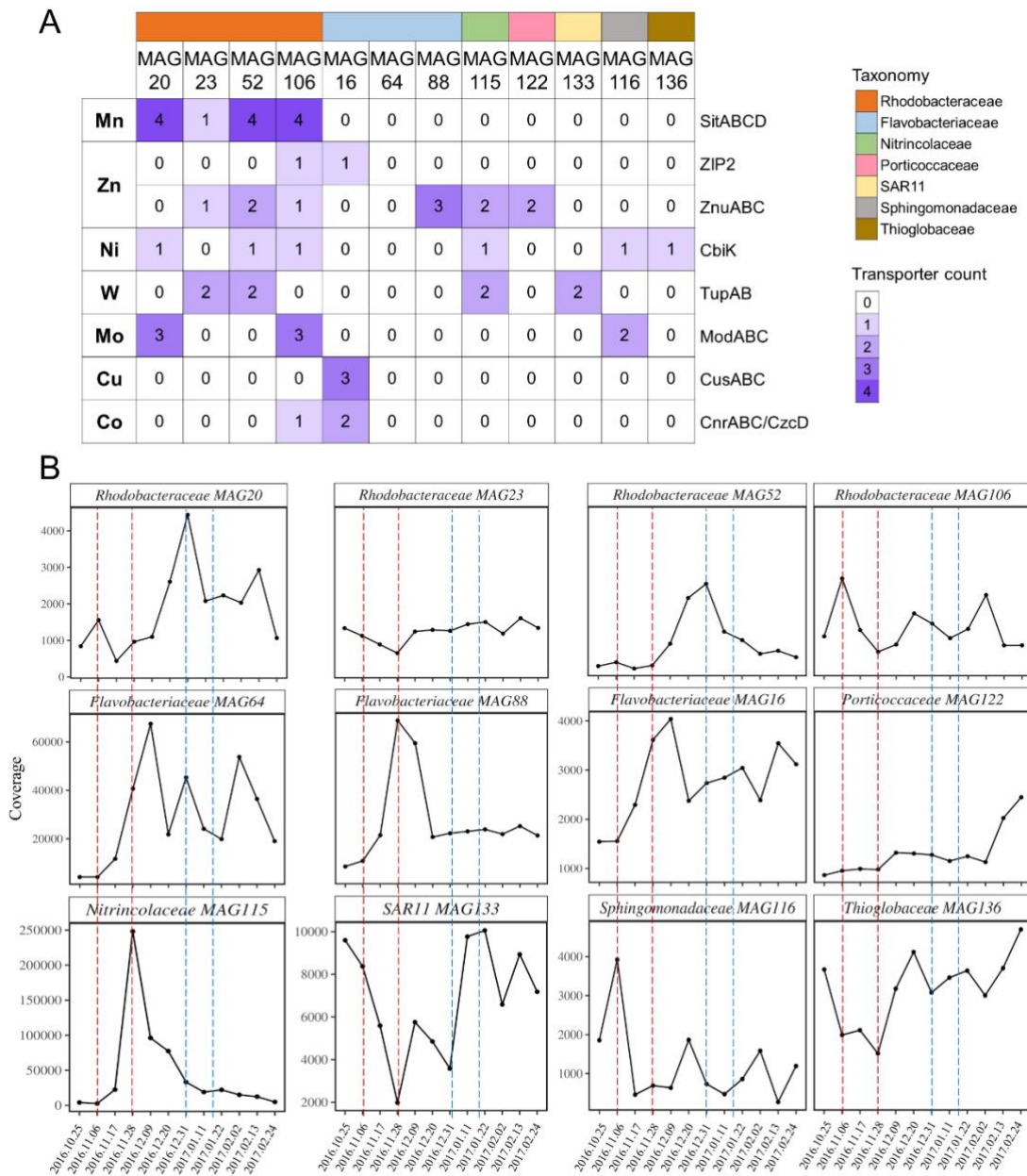


Figure 4. The distribution of specific genes related to Mn, Zn, Ni, W, Mo, Cu and Co transporters in the twelve MAGs. The square blocks are colored according to the gene counts (A). The coverage of MAGs in the twelve samples. The red lines represent the first spring phytoplankton bloom, and blue lines represent the second summer phytoplankton bloom. (B).

245

246

## 247 **Discussion**

248

249 We observed marked seasonal patterns of prokaryotic transporter genes for the metals  
250 Mn, Zn, Ni, W and Mo in the Southern Ocean. These metals are key for metalloenzymes  
251 involved in diverse metabolic pathways. Among these are pathways linked to the  
252 degradation, uptake and processing of the diverse pool of organic substrates that  
253 constitute the main source of carbon and energy for heterotrophic microbes.  
254 Concentrations of dissolved Fe (~ 0.1-0.3 nM) (Blain et al. 2007, Qu  rou   et al 2015),  
255 Mn (~ 0.3 nM; Zhang et al., under revision) are in the picomolar range in surface waters  
256 at our study site, and those of Zn (~ 2 nM) and Ni (~ 6 nM) in the lower nanomolar  
257 range (Wang et al. 2019). Mo is present at higher concentrations in marine surface water  
258 (~ 100 nM) (Matsuoka et al. 2023) than W (~ 50 pM; Matsuoka et al. 2023). Iron is  
259 essential for microbial respiration, and it has been shown that this element can be  
260 limiting for microbial growth in Southern Ocean surface waters (Obner et al.  
261 2015, Baltar et al. 2018). However, whether this is the case for the metals considered  
262 here is not known. Due to their overall higher concentrations and probably lower  
263 cellular requirements due their utilization in specific pathways, as opposed to the wider  
264 use of Fe as a redox catalyst, it is unlikely that they are direct limiting factors of  
265 microbial growth (Baltar et al. 2018). The seasonal patterns observed in our study  
266 therefore rather reflect the requirements of a given trace element for the processing of  
267 the seasonally changing amount of DOM and the diversity of organic substrates present  
268 within this pool. Our results further allow us to identify abundant prokaryotic groups  
269 with the capacity to transport a given trace element. A high contribution of a given  
270 prokaryotic group to a trace metal transporter could illustrate its competitiveness driven  
271 by trace-metal acquisition under a specific bloom stage. Given the key role of DOM in  
272 driving prokaryotic growth and community composition in this ocean region (Landa et  
273 al. 2016), we will focus our discussion on a few prominent biogeochemical processes  
274 within the marine carbon cycle involving trace metals and the potential microbial key  
275 players.

276

277 Zn and Mn are contained in enzymes with distinct roles in the cleavage and processing  
278 of organic carbon. Zn plays an important role in catalytic processes to access organic  
279 matter. About half of the Zn-bound proteins are enzymes, among which hydrolases  
280 make up more than 50% (Andreini et al. 2012). The Zn enzymes alcohol dehydrogenase  
281 and carboxypeptidase belong to glycoside hydrolase (GH) families of CAZymes, and  
282 include GH18 and GH19 responsible for the decomposition of chitin (Nguyen et al.  
283 2019). We identified both the high-affinity Zn-uptake system, encoded by the *znuABC*  
284 genes (Hantke 2001) and the low-affinity ZIP2 transporter (Grass et al. 2005). ZIP2  
285 transporters had a seasonal trend that closely matched that of CAZymes (Fig. S4)  
286 (Zhang et al. 2023) pointing to increased Zn-requirements for the degradation of  
287 complex substrates. *Flavobacteriaceae*, including *Flavobacterium* and *Polaribacter*,  
288 were the main contributors to ZIP2 (Fig. 3 and Fig. S5) and this family accounted for  
289 up to 30% of the CAZymes during the bloom decline (Zhang et al. 2023). The 3  
290 *Flavobacteriaceae* MAGs all peaked after the spring bloom (Fig. 4B) and 2 MAGs  
291 (MAG16 and MAG88) harbored genes for Zn transporters (Fig. 4A). These results  
292 highlight that *Flavobacteriaceae*, through their well-documented capacities to degrade  
293 various polymeric substrates (Xing et al. 2015; Krüger et al. 2019) could play an  
294 important role in the cycling of Zn.

295

296 Mn is involved in the central carbon metabolism, phosphorylation and peptide cleavage  
297 (Hansel 2017). Phosphoenolpyruvate synthase uses Mn as a cofactor and pyruvate  
298 carboxylase is a Mn-containing enzyme, and both are critical in gluconeogenesis  
299 (Hansel 2017). We detected the gene *sitABCD* in our metagenomes, a protein transport  
300 system that is not specific to Mn, but can potentially transport also Fe (Sabri & Dozois,  
301 2006). Using a set of transporters of Fe<sup>3+</sup> (*fbp*, *futA1/A2*, *fbpB-futB*) and Fe<sup>2+</sup> (*feo*,  
302 *efeUOB*) (Fig. S8, Zhang et al. 2023) revealed a seasonal pattern that differed from that  
303 observed for *sit* in the present study (Fig. 2A), suggesting that the temporal dynamics  
304 of *sit* likely reflect Mn transporters. The rapid increase in Mn transporters during the  
305 spring bloom and their continuously high levels throughout the declining phase is likely



306 related to the processing of readily accessible phytoplankton-derived organic substrates.  
307 *Porticoccaceae* and *Rhodobacteraceae* were identified as main contributors to *sit*  
308 transporters, but at distinct time periods (Fig. 3). The temporal pattern of the  
309 contribution of *Porticoccaceae* to *sit* transporters closely matched the dynamics of an  
310 ASV belonging to SAR92 (*Porticoccaceae*) that revealed a rapid increase in relative  
311 abundances (to up to 10%) during the spring bloom (Liu et al. 2020). These  
312 observations suggest a fast response of SAR92 to phytoplankton-derived substrates, an  
313 idea that is further supported by previous observations pointing to SAR92 as an  
314 abundant and active member of the microbial community during the peak and spring  
315 bloom decline (West et al. 2008; Obernosterer et al. 2011). Using the same  
316 metagenomic dataset, we observed that *Porticoccaceae* had a low contribution to  
317 CAZymes (2-15%) (Zhang et al. 2023), suggesting that this group had a minor  
318 implication in the degradation of complex compounds (Kim et al. 2019; He et al. 2023).  
319 *Rhodobacteraceae* accounted for a large share of *sit* transporters during the transition  
320 phase to the summer bloom consistent with the seasonal patterns of *Rhodobacteraceae*  
321 MAGs and abundant ASVs (Liu et al. 2020), suggesting their increased contribution to  
322 the processing of DOM at the final stage of the spring bloom decline (Buchan et al.  
323 2019).

324

325 Nickel is an essential cofactor of enzymes in nitrogen fixation, nitrogen uptake and  
326 carbon fixation. Among nickel-dependent enzymes are urease, carbon monoxide  
327 dehydrogenase (CODH) and superoxide dismutase (NiSOD). *Nitriolaceae* had a  
328 dominant contribution to the Ni transporters *cbik* during the early spring bloom decline  
329 when the respective GPMs were high (Fig. 2). This pattern could be due to the presence  
330 of two *Nitriolaceae* ASVs that together reached 40% relative abundance (Liu et al.  
331 2020), coherent with the remarkably high coverage of *Nitriolaceae* MAG115 that  
332 harbored *cbik* (Fig. 4). *Nitriolaceae* are specialized in the utilization of amino acids  
333 and peptides (Francis et al. 2021; Debeljak et al. 2023) which could explain the high  
334 contribution of this family to the peptide/nickel transport system in early spring (*ddp*,  
335 PE.P, PE.P1, PE.S) (Fig. S6A). Urea is a nitrogen containing compound and its

336 utilization requires the Ni-containing enzyme urease. Urea can account for a substantial  
337 fraction of the prokaryotic nitrogen demand in marine systems (Jørgensen 2006),  
338 including the Southern Ocean (Hollibaugh et al. 2023) and diverse prokaryotic taxa are  
339 implicated in this process (Connelly et al. 2014). The increase in the concentrations of  
340 ammonium during the bloom decline (Fig. S1) could indicate that reduced forms of  
341 nitrogen, including urea, become important sources of this nutrient for certain  
342 prokaryotes, potentially including *Nitri-colaceae*. Further in-depth studies are required  
343 to confirm this idea.

344

345 Tungstoenzymes are required by methylotrophic prokaryotes to metabolize organic  
346 substrates containing no carbon-carbon bonds, such as single-carbon (C1) compounds  
347 (e.g. methane, methanol), methylated amines and methylated sulfur species (DMS,  
348 DMSO) by specialized pathways (Chistoserdova 2011; Maia et al. 2017). W-containing  
349 formate dehydrogenase (FDH) catalyzes the oxidation of formate, an intermediate  
350 product in methylotrophy, to carbon dioxide and therefore plays an important role in  
351 the processing of these compounds (Chistoserdova 2011). Methylotrophy appears to be  
352 widespread in marine microbial communities (Sun et al. 2011; Lidbury et al. 2014). In  
353 the present study, *Rhodobacteraceae* were the main contributors to W-transporters  
354 throughout the season, except for the peak of the spring bloom when W-transporters  
355 were mainly affiliated with *Nitri-colaceae* (Fig.3). *Rhodobacteraceae* are known  
356 utilizers of methylated sulfur compounds (Buchan et al. 2005) and amines (Chen 2012;  
357 Lidbury et al. 2014, Taubert et al. 2017), which could explain their W requirements.  
358 Recent observations point to a potential role of *Nitri-colaceae* in C1 metabolism  
359 (Francis et al. 2021). The full set of methanesulfonate monooxygenase genes, required  
360 for the utilization of methanesulfonate as carbon source and for the oxidation of DMS  
361 were present and expressed in *Nitri-colaceae* MAGs from the Southern North Sea  
362 (Francis et al. 2021). These observations could point to a possible role of *Nitri-colaceae*  
363 members in methylotrophy, but further genome-based investigations would be required  
364 to identify the pathways involving W-containing enzymes in members belonging to this  
365 family.

366

367 Mo is widely known for its role in nitrogenase, the enzyme responsible for N<sub>2</sub> fixation  
368 (Tuit, 2003). Another metabolism in which Mo is involved is carbon monoxide (CO)  
369 oxidation. Mo-containing CO dehydrogenase (CODH, *coxSML*) is an enzyme in  
370 aerobic CO oxidizers that can use CO as their carbon source (King and Weber, 2007).  
371 The seasonal trend in Mo transporters, peaking in late summer, matched those of *nifH*  
372 and CODH (Fig. S4) and suggests that both pathways could potentially be taking place.  
373 The main contributors to the *nifH* genes were *Xanthobacteraceae* (Fig. S6C), a family  
374 that is widely known to have N<sub>2</sub> fixing capacity (Brenner et al. 2005; González-Cortés  
375 et al. 2022). *Thioglobaceae*, important contributors to Mo transporters throughout the  
376 season, have the potential for carbon fixation (Morris et al. 2022), however, in the  
377 present study *cox* was not affiliated with this group. By contrast, *Rhodobacteraceae*  
378 contributed to both *mod* and *cox*, suggesting that members of this group could make  
379 use of this pathway. Genomic insights (Moran et al. 2004, Simon et al. 2017) and uptake  
380 experiments (Tolli et al. 2006) have shown that *Roseobacter* oxidize CO. These Mo-  
381 requiring processes are likely to occur concurrently, but carried out by different  
382 microbial groups.

383

384 Several trace metals could further play a role in superoxide dismutases (SODs). SODs  
385 are metalloenzymes that catalyze the conversion of superoxide molecules to hydrogen  
386 peroxide and molecular oxygen. SODs are one of the main defense mechanisms of cells  
387 against oxidative stress (McCord and Fridovich, 1969). Three types of SODs were  
388 described in prokaryotes, that are Ni-containing SODs (NiSOD), Fe- or Mn-containing  
389 SODs (FeSOD and MnSOD), and Cu- and Zn-containing SODs (Cu,ZnSODs) (Wang  
390 et al. 2018). In our metagenomes, all types of SODs were identified and they peaked  
391 during the early spring bloom decline (Fig. S7). Microbial respiration is linked to the  
392 formation of reactive oxygen species (ROS) that can be neutralized by SODs (Tiwari  
393 et al. 2002). The sharp increase in SODs could be a result of the enhanced microbial  
394 metabolism in response to the phytoplankton bloom, including respiration of large

395 amounts of DOM (Lesser 2006). Our results indicate that different metals could be used  
396 for SODs concurrently. The involvement of diverse taxa in this key process in  
397 combination with the different capacities of these prokaryotes of transport metals could  
398 explain this pattern.

399

400 The seasonal dynamics of the contribution of prokaryotic groups to trace metal  
401 transporters as observed in the present study point to distinct capabilities in the  
402 acquisition of these elements. In combination with the temporal trends in the  
403 abundances of a given trace metal transporter, our findings provide insights to the  
404 potential roles of abundant prokaryotic groups in the cycling of trace metals during  
405 consecutive spring and summer phytoplankton blooms in the Southern Ocean.  
406 *Rhodobacteraceae* had a broad repertoire of trace metal transporters (Mn, Zn, Ni, W,  
407 Mo) a feature that likely reflects the large diversity of metabolic functions present in  
408 this prokaryotic group. Our data suggest a more restricted repertoire for  
409 *Flavobacteriaceae* (Zn) and *Nitrospiraceae* (Ni, W), which could point to a more  
410 specialized functional role possibly associated with requirements of a reduced set of  
411 trace metals. The temporal variability in the abundances of genes encoding for trace  
412 metal transporters provides insight on the bloom stages that are favorable for diverse  
413 metal-requiring pathways to occur. Our results, based on trace metal transporter  
414 capacities, represent a novel perspective on the functional role of prokaryotes in the  
415 biogeochemical cycling of elements in the ocean.

416

#### 417 **Author contributions**

418 Yanhui Kong, Stephane Blain and Ingrid Obernosterer designed the research.  
419 Bioinformatic analyses were performed by Yanhui Kong and Rui Zhang. Yanhui Kong  
420 and Ingrid Obernosterer wrote the first draft of the manuscript. All authors contributed  
421 to editing the manuscript.

#### 422 **Acknowledgements**

423 We thank the team of the Technical Division of the Institute of the Sciences of the  
424 Universe (DT-INSU) for the design and construction of the mooring for the RAS. We  
425 thank the captains and the crews of the R/V Marion Dufresne for their support during  
426 the deployment and the recovery of the RAS. The project SOCLIM (Southern Ocean  
427 and Climate) was supported by the Climate Initiative of the BNP Paribas Foundation,  
428 the French Polar Institute (Institut Polaire Paul Emile Victor), and the French program  
429 LEFE-CYBER of the CNRS-INSU. We thank Yan Liu who carried out the DNA  
430 extraction. We thank the French Institute of Bioinformatics (IFB; [https://www.france-](https://www.france-bioinformatique.fr)  
431 [bioinformatique.fr](https://www.france-bioinformatique.fr)) for providing computing resources. The insightful comments of 3  
432 reviewers helped improve a previous version of the manuscript. This work is part of  
433 the PhD thesis of Y.K. supported by the China Scholarship Council (CSC; No.  
434 202106230202).

#### 435 **Competing interests**

436 The authors declare no competing interests.

#### 437 **Data availability statement**

438 The data sets generated and analyzed during the current study are available in the  
439 European Nucleotide Archive (ENA) repository at <https://www.ebi.ac.uk/ena> under  
440 the project ID PRJEB56376.

441 **References**

442

443 Andreini, C., and Bertini, I. (2012). A bioinformatics view of zinc enzymes. *Journal of*  
444 *inorganic biochemistry*, **111**, 150-156.

445 Argüello, J. M., Raimunda, D., & Padilla-Benavides, T. (2013). Mechanisms of copper  
446 homeostasis in bacteria. *Frontiers in cellular and infection microbiology*, **3**, 73.

447 Baltar, F., Gutiérrez-Rodríguez, A., Skudelny, I., Sander, S., Nodder, S., & Morales, S.  
448 E. (2018). Specific effect of trace metals on marine heterotrophic microbial  
449 activity and diversity: Key role of iron and zinc and hydrocarbon-degrading  
450 bacteria. *Frontiers in Microbiology*, **9**, 420958.

451 Bertrand, E. M., McCrow, J. P., Moustafa, A., Zheng, H., McQuaid, J. B., Delmont, T.  
452 O., ... & Allen, A. E. (2015). Phytoplankton-bacterial interactions mediate  
453 micronutrient colimitation at the coastal Antarctic Sea ice edge. *Proceedings of the*  
454 *National Academy of Sciences*, **112**(32), 9938-9943.

455 Blain, S., Queguiner, B., Armand, L., Belviso, S., Bombled, B., Bopp, L., ... & Wagener,  
456 T. (2007). Effect of natural iron fertilization on carbon sequestration in the  
457 Southern Ocean. *Nature*, **446**(7139), 1070-1074.

458 Blain, S., Rembauville, M., Crispi, O., & Obernosterer, I. (2021). Synchronized  
459 autonomous sampling reveals coupled pulses of biomass and export of  
460 morphologically different diatoms in the Southern Ocean. *Limnology and*  
461 *Oceanography*, **66**(3), 753-764.

462 Brenner, D. J., Krieg, N. R., Staley, J. T., Garrity, G. M., Boone, D. R., Vos, P. D., ... &  
463 Schleifer, K. H. (2005). Bergey's manual of systematic bacteriology: the  
464 proteobacteria; part B: the gammaproteobacteria. In *Bergey's manual of systematic*  
465 *bacteriology: the proteobacteria; part B: the gammaproteobacteria* (pp. 1106-  
466 1106).

467 Buchan, A., González, J. M., & Chua, M. J. (2019). Aerobic Hydrocarbon-Degrading  
468 Alphaproteobacteria: Rhodobacteraceae (Roseobacter). *Taxonomy, genomics and*  
469 *ecophysiology of hydrocarbon-degrading microbes*, 93-104.

470 Buchan, A., González, J. M., & Moran, M. A. (2005). Overview of the marine  
471 Roseobacter lineage. *Applied and environmental microbiology*, **71**(10), 5665-5677.

472 Chen, Y. (2012). Comparative genomics of methylated amine utilization by marine  
473 Roseobacter clade bacteria and development of functional gene markers (tmm,  
474 gmaS). *Environmental microbiology*, **14**(9), 2308-2322.

475 Chistoserdova, L. (2011). Modularity of methylotrophy, revisited. *Environmental*  
476 *microbiology*, **13**(10), 2603-2622.

477 Connelly, T. L., Baer, S. E., Cooper, J. T., Bronk, D. A., & Wawrik, B. (2014). Urea  
478 uptake and carbon fixation by marine pelagic bacteria and archaea during the  
479 Arctic summer and winter seasons. *Applied and environmental microbiology*,  
480 **80**(19), 6013-6022.

481 Debeljak, P., Bayer, B., Sun, Y., Herndl, G. J., & Obernosterer, I. (2023). Seasonal  
482 patterns in microbial carbon and iron transporter expression in the Southern Ocean.  
483 *Microbiome*, **11**(1), 187.

484 Debeljak, P., Blain, S., Bowie, A., van der Merwe, P., Bayer, B., & Obernosterer, I.  
485 (2021). Homeostasis drives intense microbial trace metal processing on marine  
486 particles. *Limnology and Oceanography*, **66**(10), 3842-3855.

487 Debeljak, P., Toulza, E., Beier, S., Blain, S., & Obernosterer, I. (2019). Microbial iron  
488 metabolism as revealed by gene expression profiles in contrasted Southern Ocean  
489 regimes. *Environmental Microbiology*, **21**(7), 2360-2374.

490 Francis, B., Urich, T., Mikolasch, A., Teeling, H., & Amann, R. (2021). North Sea  
491 spring bloom-associated Gammaproteobacteria fill diverse heterotrophic niches.  
492 *Environmental Microbiome*, **16**, 1-16.

493 Franke, S., Grass, G., Rensing, C., & Nies, D. H. (2003). Molecular analysis of the  
494 copper-transporting efflux system CusCFBA of *Escherichia coli*. *Journal of*  
495 *bacteriology*, **185**(13), 3804-3812.

496 González-Cortés, J. J., Valle, A., Ramírez, M., & Cantero, D. (2022). Characterization  
497 of bacterial and Archaeal communities by DGGE and next generation sequencing  
498 (NGS) of nitrification bioreactors using two different intermediate landfill

499 leachates as ammonium substrate. *Waste and Biomass Valorization*, **13**(9), 3753-  
500 3766.

501 Grass, G., Franke, S., Taudte, N., Nies, D. H., Kucharski, L. M., Maguire, M. E., &  
502 Rensing, C. (2005). The metal permease ZupT from *Escherichia coli* is a  
503 transporter with a broad substrate spectrum. *Journal of bacteriology*, **187**(5),  
504 1604-1611.

505 Grunden, A. M., & Shanmugam, K. T. (1997). Molybdate transport and regulation in  
506 bacteria. *Archives of microbiology*, **168**, 345-354.

507 Hagen, W. R. (2023). The Development of Tungsten Biochemistry—A Personal  
508 Recollection. *Molecules*, **28**(10), 4017.

509 Hansel, C. M. (2017). Manganese in marine microbiology. *Advances in microbial*  
510 *physiology*, **70**, 37-83.

511 Hantke, K. (2001). Bacterial zinc transporters and regulators. *Zinc Biochemistry,*  
512 *Physiology, and Homeostasis: Recent Insights and Current Trends*, 53-63.

513 He, X. Y., Liu, N. H., Liu, J. Q., Peng, M., Teng, Z. J., Gu, T. J., ... & Zhang, X. Y.  
514 (2023). SAR92 clade bacteria are potentially important DMSP degraders and  
515 sources of climate-active gases in marine environments. *mBio*, **14**(6), e01467-23.

516 Hobbs, E. E., Gloster, T. M., & Pritchard, L. (2023). cazy\_webscraper: local  
517 compilation and interrogation of comprehensive CAZyme datasets. *Microbial*  
518 *Genomics*, **9**(8), 001086.

519 Hogle, S. L., Thrash, J. C., Dupont, C. L., & Barbeau, K. A. (2016). Trace metal  
520 acquisition by marine heterotrophic bacterioplankton with contrasting trophic  
521 strategies. *Applied and Environmental Microbiology*, **82**(5), 1613-1624.

522 Hollibaugh, J. T., Okotie-Oyekan, A., Damashek, J., H Ducklow, H., Popp, B. N.,  
523 Wallsgrove, N., & Allen, T. (2023). Contribution of urea-N to nitrification in the  
524 Southern Ocean west of the Antarctic Peninsula. *Applied and environmental*  
525 *microbiology*.

526 Hopkinson, B. M., & Barbeau, K. A. (2012). Iron transporters in marine prokaryotic  
527 genomes and metagenomes. *Environmental microbiology*, **14**(1), 114-128.



528 Huerta-Cepas, J., Szklarczyk, D., Heller, D., Hernández-Plaza, A., Forslund, S. K.,  
529 Cook, H., ... & Bork, P. (2019). eggNOG 5.0: a hierarchical, functionally and  
530 phylogenetically annotated orthology resource based on 5090 organisms and 2502  
531 viruses. *Nucleic acids research*, **47**(D1), D309-D314.

532 Hyatt, D., Chen, G. L., LoCascio, P. F., Land, M. L., Larimer, F. W., & Hauser, L. J.  
533 (2010). Prodigal: prokaryotic gene recognition and translation initiation site  
534 identification. *BMC bioinformatics*, **11**, 1-11.

535 Jørgensen, N. O. (2006). Uptake of urea by estuarine bacteria. *Aquatic Microbial  
536 Ecology*, **42**(3), 227-242.

537 Kanehisa, M., Sato, Y., & Morishima, K. (2016). BlastKOALA and GhostKOALA:  
538 KEGG tools for functional characterization of genome and metagenome  
539 sequences. *Journal of molecular biology*, **428**(4), 726-731.

540 Kim, D., Song, L., Breitwieser, F. P., & Salzberg, S. L. (2016). Centrifuge: rapid and  
541 sensitive classification of metagenomic sequences. *Genome research*, **26**(12),  
542 1721-1729.

543 Kim, S. J., Kim, J. G., Lee, S. H., Park, S. J., Gwak, J. H., Jung, M. Y., ... & Rhee, S.  
544 K. (2019). Genomic and metatranscriptomic analyses of carbon remineralization  
545 in an Antarctic polynya. *Microbiome*, **7**, 1-15.

546 King, G. M., & Weber, C. F. (2007). Distribution, diversity and ecology of aerobic CO-  
547 oxidizing bacteria. *Nature Reviews Microbiology*, **5**(2), 107-118.

548 Krüger, K., Chafee, M., Ben Francis, T., Glavina del Rio, T., Becher, D., Schweder,  
549 T., ... & Teeling, H. (2019). In marine Bacteroidetes the bulk of glycan degradation  
550 during algae blooms is mediated by few clades using a restricted set of genes. *The  
551 ISME journal*, **13**(11), 2800-2816.

552 Kuypers, M. M., Marchant, H. K., & Kartal, B. (2018). The microbial nitrogen-cycling  
553 network. *Nature Reviews Microbiology*, **16**(5), 263-276.

554 Landa, M., Blain, S., Christaki, U., Monchy, S., & Obernosterer, I. (2016). Shifts in  
555 bacterial community composition associated with increased carbon cycling in a  
556 mosaic of phytoplankton blooms. *The ISME journal*, **10**(1), 39-50.

557 Langmead, B., & Salzberg, S. L. (2012). Fast gapped-read alignment with Bowtie 2.  
558 *Nature methods*, **9**(4), 357-359.

559 Leaden, L., Silva, L. G., Ribeiro, R. A., Lorenzetti, A. P., Koide, T., & Marques, M. V.  
560 (2018). Iron deficiency generates oxidative stress and activation of the SOS  
561 response in *Caulobacter crescentus*. *Frontiers in microbiology*, **9**, 381348.

562 Lesser, M. P. (2006). Oxidative stress in marine environments: biochemistry and  
563 physiological ecology. *Annu. Rev. Physiol.*, **68**, 253-278.

564 Li, W., & Godzik, A. (2006). Cd-hit: a fast program for clustering and comparing large  
565 sets of protein or nucleotide sequences. *Bioinformatics*, **22**(13), 1658-1659.

566 Lidbury, I., Murrell, J. C., & Chen, Y. (2014). Trimethylamine N-oxide metabolism by  
567 abundant marine heterotrophic bacteria. *Proceedings of the National Academy of*  
568 *Sciences*, **111**(7), 2710-2715.

569 Liu, Y., Blain, S., Crispi, O., Rembauville, M. & Obernosterer, I. (2020) Seasonal  
570 dynamics of prokaryotes and their associations with diatoms in the Southern  
571 Ocean as revealed by an autonomous sampler. *Environmental Microbiology*, **22**,  
572 3968-3984.

573 Maia, L. B., Moura, I., & Moura, J. J. (2017). Molybdenum and tungsten-containing  
574 formate dehydrogenases: Aiming to inspire a catalyst for carbon dioxide utilization.  
575 *Inorganica Chimica Acta*, **455**, 350-363.

576 Matsuoka, K., Tatsuyama, T., Takano, S., & Sohrin, Y. (2023). Distribution of stable  
577 isotopes of Mo and W from a river to the ocean: signatures of anthropogenic  
578 pollution. *Frontiers in Marine Science*, **10**, 1182668.

579 McCord, J. M., & Fridovich, I. (1969). Superoxide dismutase: an enzymic function for  
580 erythrocyte hemocuprein (hemocuprein). *Journal of Biological chemistry*, **244**(22), 6049-  
581 6055.

582 Moran, M. A., Buchan, A., González, J. M., Heidelberg, J. F., Whitman, W. B., Kiene,  
583 R. P., ... & Ward, N. (2004). Genome sequence of *Silicibacter pomeroyi* reveals  
584 adaptations to the marine environment. *Nature*, **432**(7019), 910-913.

585 Morris, R. M., and Spietz, R. L. (2022). The physiology and biogeochemistry of SUP05.  
586 *Annual Review of Marine Science*, **14**, 261-275.

587 Nguyen, S. N., Flores, A., Talamantes, D., Dar, F., Valdez, A., Schwans, J., & Berlemont,  
588 R. (2019). GeneHunt for rapid domain-specific annotation of glycoside hydrolases.  
589 *Scientific Reports*, **9**(1), 10137.

590 Nurk, S., Meleshko, D., Korobeynikov, A., & Pevzner, P. A. (2017). metaSPAdes: a  
591 new versatile metagenomic assembler. *Genome research*, **27**(5), 824-834.

592 Obernosterer, I., Catala, P., Lebaron, P., & West, N. J. (2011). Distinct bacterial groups  
593 contribute to carbon cycling during a naturally iron fertilized phytoplankton bloom  
594 in the Southern Ocean. *Limnology and oceanography*, **56**(6), 2391-2401.

595 Obernosterer, I., Fourquez, M., & Blain, S. (2015). Fe and C co-limitation of  
596 heterotrophic bacteria in the naturally fertilized region off the Kerguelen Islands.  
597 *Biogeosciences*, **12**(6), 1983-1992.

598 Okamoto, S., & Eltis, L. D. (2011). The biological occurrence and trafficking of cobalt.  
599 *Metallomics*, **3**(10), 963-970.

600 Papp-Wallace, K. M., & Maguire, M. E. (2006). Manganese transport and the role of  
601 manganese in virulence. *Annu. Rev. Microbiol.*, **60**, 187-209.

602 Parks, D. H., Chuvochina, M., Rinke, C., Mussig, A. J., Chaumeil, P. A., & Hugenholtz,  
603 P. (2022). GTDB: an ongoing census of bacterial and archaeal diversity through a  
604 phylogenetically consistent, rank normalized and complete genome-based  
605 taxonomy. *Nucleic acids research*, **50**(D1), D785-D794.

606 Qu erou , F., Sarthou, G., Planquette, H. F., Bucciarelli, E., Chever, F., van Der Merwe,  
607 P., ... & Bowie, A. R. (2015). High variability in dissolved iron concentrations in  
608 the vicinity of the Kerguelen Islands (Southern Ocean). *Biogeosciences*, **12**(12),  
609 3869-3883.

610 Ridge, P. G., Zhang, Y., & Gladyshev, V. N. (2008). Comparative genomic analyses of  
611 copper transporters and cuproproteomes reveal evolutionary dynamics of copper  
612 utilization and its link to oxygen. *PLoS One*, **3**(1), e1378.

613 Rodionov, D. A., Hebbeln, P., Gelfand, M. S., & Eitinger, T. (2006). Comparative and  
614 functional genomic analysis of prokaryotic nickel and cobalt uptake transporters:  
615 evidence for a novel group of ATP-binding cassette transporters. *Journal of*  
616 *bacteriology*, **188**(1), 317-327.

617 Sabri, M., Leveille, S., & Dozois, C. M. (2006). A SitABCD homologue from an avian  
618 pathogenic *Escherichia coli* strain mediates transport of iron and manganese and  
619 resistance to hydrogen peroxide. *Microbiology*, **152**(3), 745-758.

620 Simon, M., Scheuner, C., Meier-Kolthoff, J. P., Brinkhoff, T., Wagner-Döbler, I.,  
621 Ulbrich, M., ... & Göker, M. (2017). Phylogenomics of Rhodobacteraceae reveals  
622 evolutionary adaptation to marine and non-marine habitats. *The ISME journal*,  
623 **11**(6), 1483-1499.

624 Sun, J., Steindler, L., Thrash, J. C., Halsey, K. H., Smith, D. P., Carter, A. E., ... &  
625 Giovannoni, S. J. (2011). One carbon metabolism in SAR11 pelagic marine  
626 bacteria. *PloS one*, **6**(8), e23973.

627 Sun, Y., Debeljak, P., & Obernosterer, I. (2021). Microbial iron and carbon metabolism  
628 as revealed by taxonomy-specific functional diversity in the Southern Ocean. *The*  
629 *ISME Journal*, **15**(10), 2933-2946.

630 Taubert, M., Grob, C., Howat, A. M., Burns, O. J., Pratscher, J., Jehmlich, N., ... &  
631 Murrell, J. C. (2017). Methylamine as a nitrogen source for microorganisms from  
632 a coastal marine environment. *Environmental microbiology*, **19**(6), 2246-2257.

633 Teeling, H., Fuchs, B. M., Becher, D., Klockow, C., Gardebrecht, A., Bennke, C. M., ...  
634 & Amann, R. (2012). Substrate-controlled succession of marine bacterioplankton  
635 populations induced by a phytoplankton bloom. *Science*, **336**(6081), 608-611.

636 Tiwari, B. S., Belenghi, B., & Levine, A. (2002). Oxidative stress increased respiration  
637 and generation of reactive oxygen species, resulting in ATP depletion, opening of  
638 mitochondrial permeability transition, and programmed cell death. *Plant*  
639 *physiology*, **128**(4), 1271-1281.

640 Tolli, J. D., Sievert, S. M., & Taylor, C. D. (2006). Unexpected diversity of bacteria  
641 capable of carbon monoxide oxidation in a coastal marine environment, and  
642 contribution of the Roseobacter-associated clade to total CO oxidation. *Applied*  
643 *and Environmental Microbiology*, **72**(3), 1966-1973.

644 Tuit, C. B. (2003). *The marine biogeochemistry of molybdenum* (Doctoral dissertation,  
645 Massachusetts Institute of Technology).

646 Wang, R. M., Archer, C., Bowie, A. R., & Vance, D. (2019). Zinc and nickel isotopes  
647 in seawater from the Indian Sector of the Southern Ocean: the impact of natural  
648 iron fertilization versus Southern Ocean hydrography and biogeochemistry.  
649 *Chemical Geology*, 511, 452-464.

650 Wang, Y., Branicky, R., Noë, A., & Hekimi, S. (2018). Superoxide dismutases: Dual  
651 roles in controlling ROS damage and regulating ROS signaling. *Journal of Cell*  
652 *Biology*, 217(6), 1915-1928.

653 West, N. J., Obernosterer, I., Zemb, O., & Lebaron, P. (2008). Major differences of  
654 bacterial diversity and activity inside and outside of a natural iron-fertilized  
655 phytoplankton bloom in the Southern Ocean. *Environmental Microbiology*, **10**(3),  
656 738-756.

657 Xing, P., Hahnke, R. L., Unfried, F., Markert, S., Huang, S., Barbeyron, T., ... & Teeling,  
658 H. (2015). Niches of two polysaccharide-degrading *Polaribacter* isolates from the  
659 North Sea during a spring diatom bloom. *The ISME journal*, **9**(6), 1410-1422.

660 Zhang, R., Debeljak, P., Blain, S., & Obernosterer, I. (2023). Seasonal shifts in Fe-  
661 acquisition strategies in Southern Ocean microbial communities revealed by  
662 metagenomics and autonomous sampling. *Environmental Microbiology*, **25**(10),  
663 1816-1829.

664

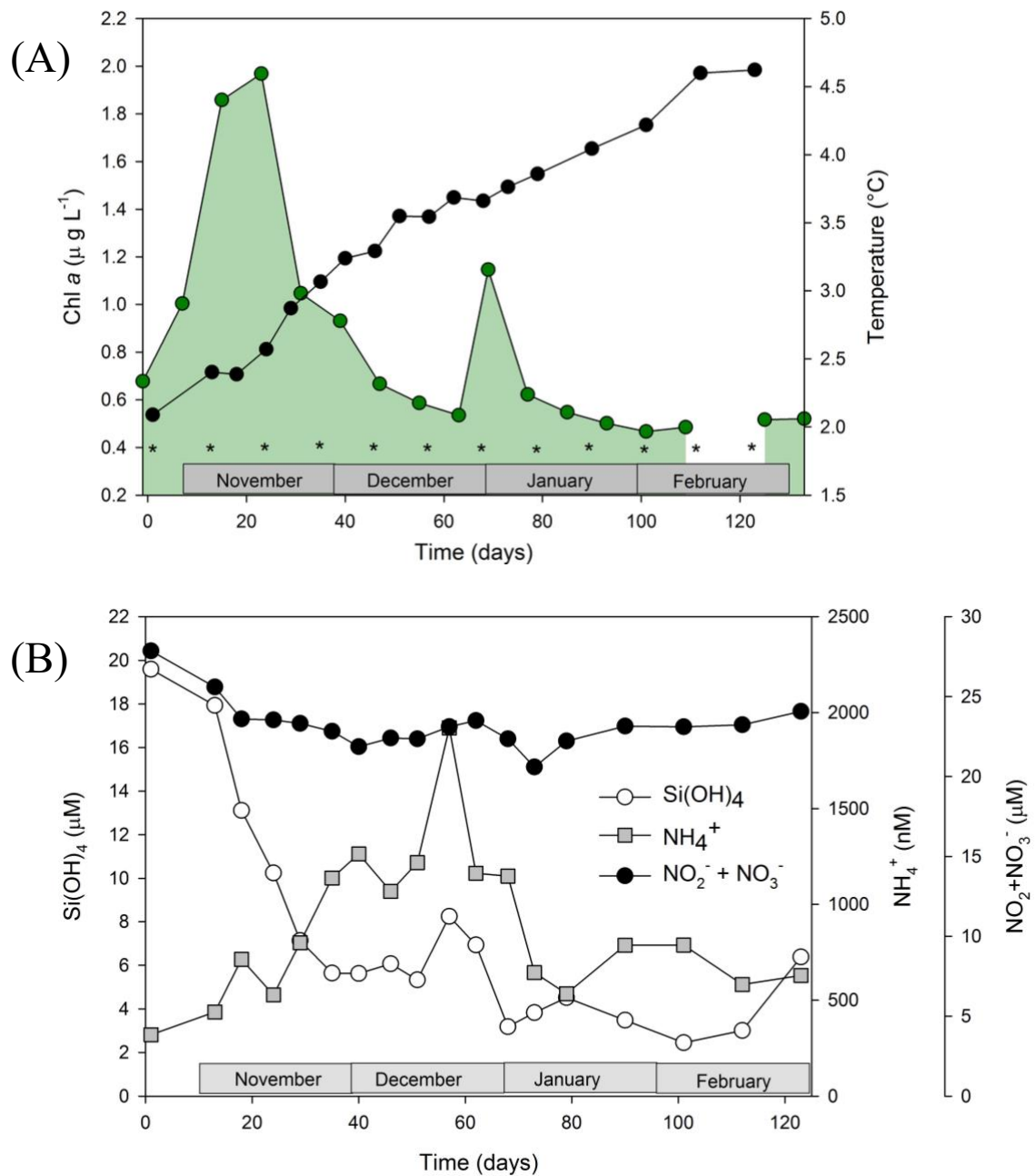
**Supplementary Information for**  
**“Seasonal dynamics in microbial trace metals transporters during**  
**phytoplankton blooms in the Southern Ocean”**

Yanhui Kong<sup>1,2</sup>, Rui Zhang<sup>2</sup>, Stéphane Blain<sup>2</sup>, Ingrid Obernosterer<sup>2</sup>

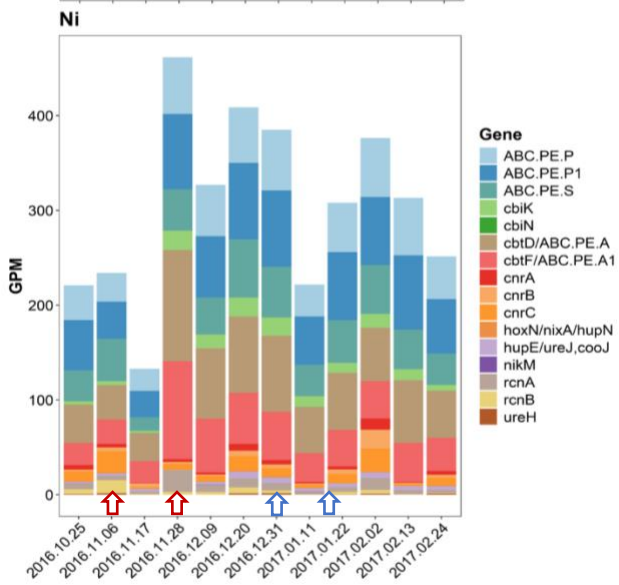
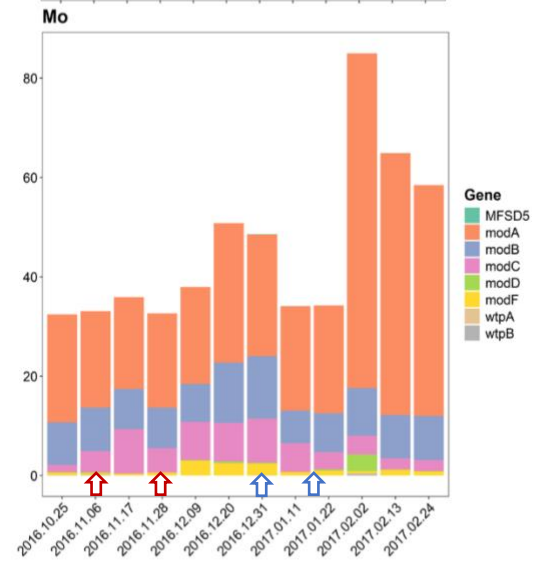
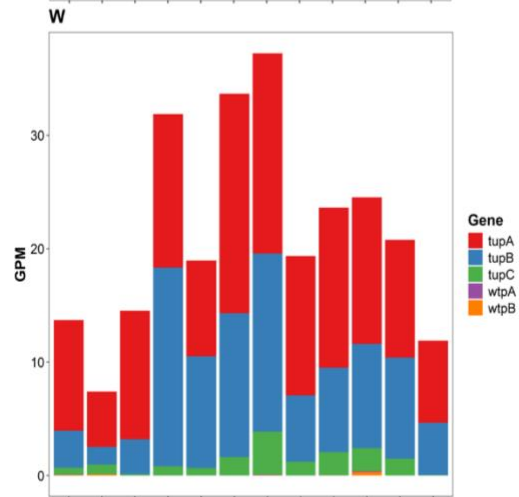
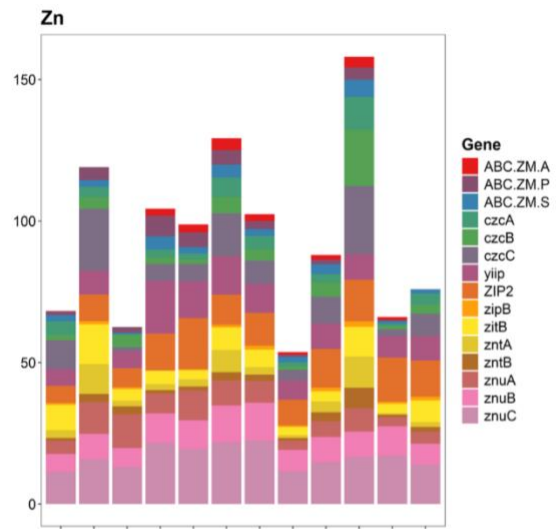
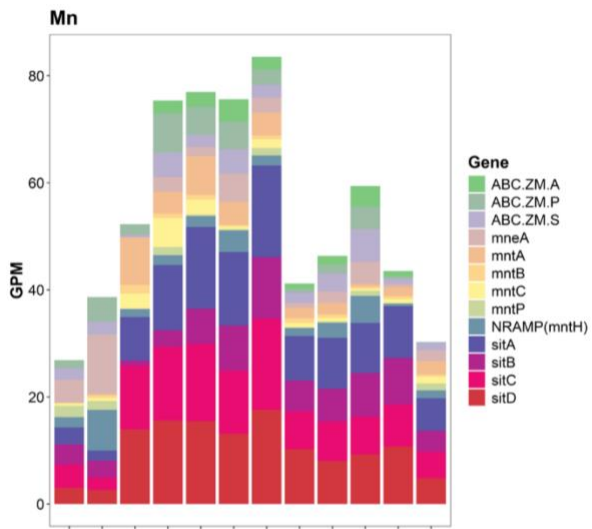
Affiliations

1 - School of Oceanography, Shanghai Jiao Tong University, 1954 Huashan Rd.,  
Shanghai 200030, China

2 - Sorbonne Université, CNRS, Laboratoire d'Océanographie Microbienne, LOMIC,  
Banyuls-sur-Mer, France



**Figure S1** Temporal changes of Chlorophyll *a* (green shaded area) and temperature (black circles) during the period of RAS deployment (A). Temporal changes of silicic acid ( $\text{Si(OH)}_4$ ), ammonium ( $\text{NH}_4^+$ ) and nitrite+nitrate ( $\text{NO}_2^- + \text{NO}_3^-$ ) during the period of sampling (25 October 2016 to 24 February 2017) (B). Data are from Blain *et al.* (2021).





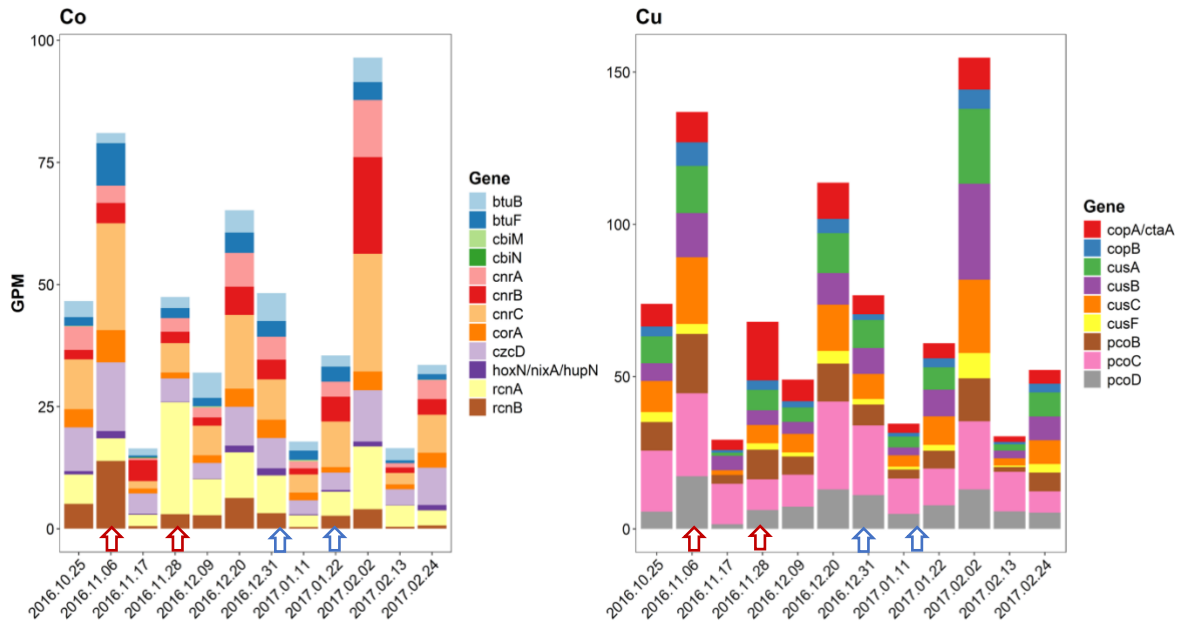


**Figure S2** Abundance of genes related to Mn, Zn, W, Mo, Ni, Co and Cu transport at the 12 time points. Gene abundance is represented by genes per kilobase million (GPM). Red arrows indicate the first spring phytoplankton bloom, and blue arrows indicate the second summer phytoplankton bloom.

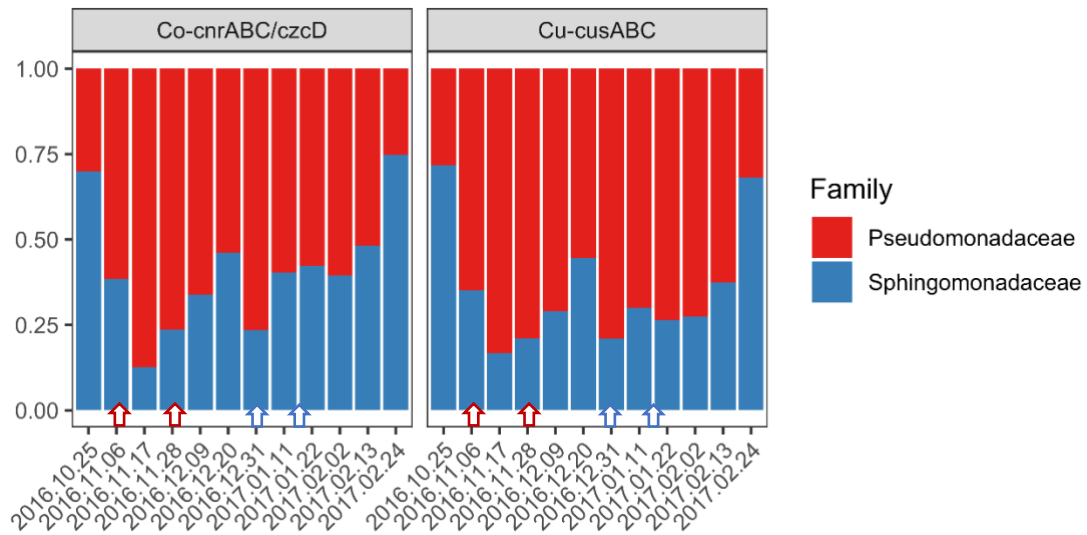


**Figure S3** Relative contribution of prokaryotic groups to specific genes associated with Co and Cu efflux transporters. Prokaryotic groups are based on the family level. Red arrows indicate the first spring phytoplankton bloom, and blue arrows indicate the second summer phytoplankton bloom.

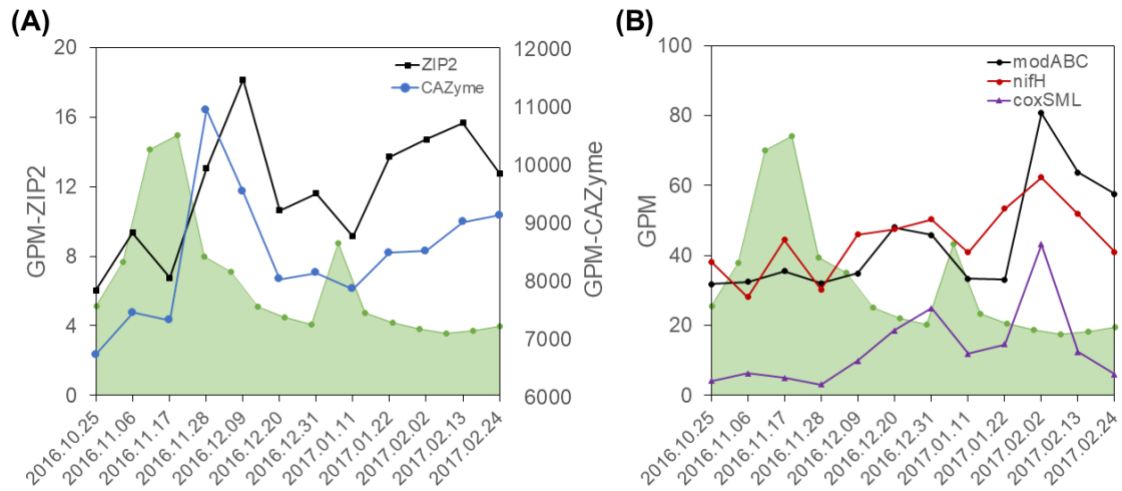


**Figure S4** Temporal changes of Chlorophyll a (green shaded area) and abundance of genes for Zn transporter (ZIP2) and carbohydrate-active enzymes (CAZymes) (**A**), Mo transporters (*modABC*), nitrogen fixation gene (*nifH*) and carbon monoxide dehydrogenase (*coxSML*) (**B**). Normalized gene abundances are given in genes per kilobase million (GPM).

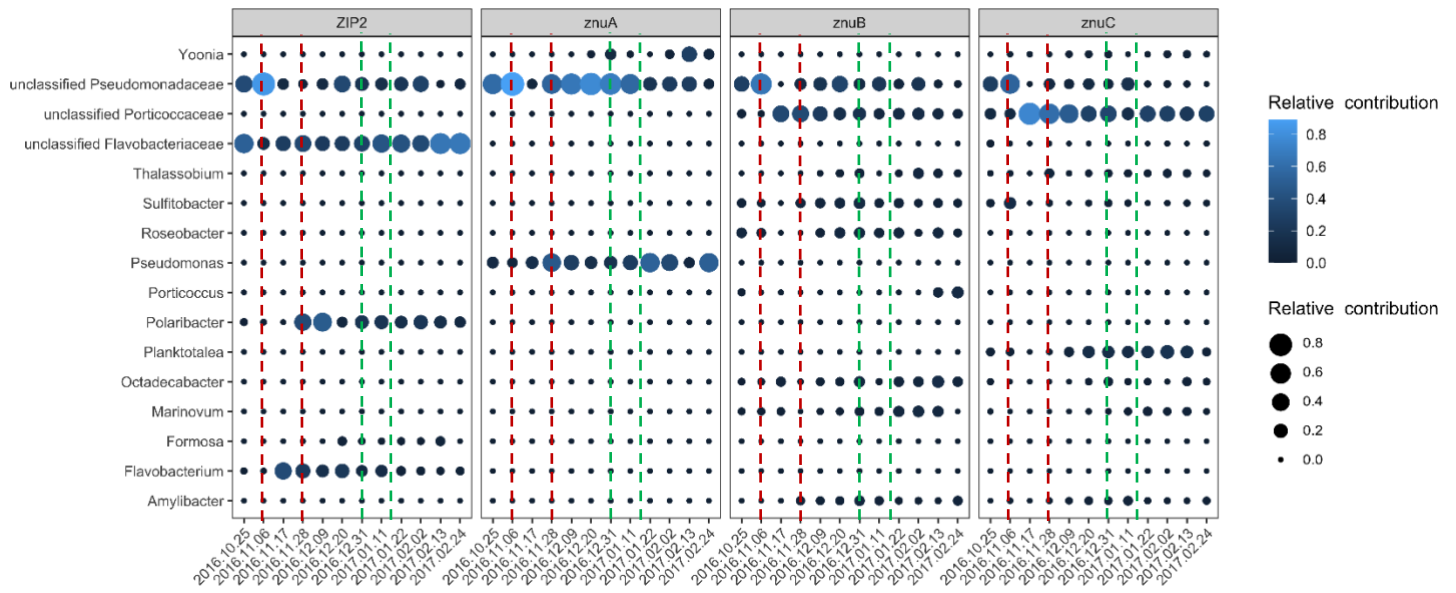


**Figure S5** Relative contribution of prokaryotic groups to specific genes associated with Zn transport. Prokaryotic groups are based on the genus level. The red lines represent the first spring phytoplankton bloom, and green lines represent the second summer phytoplankton bloom.

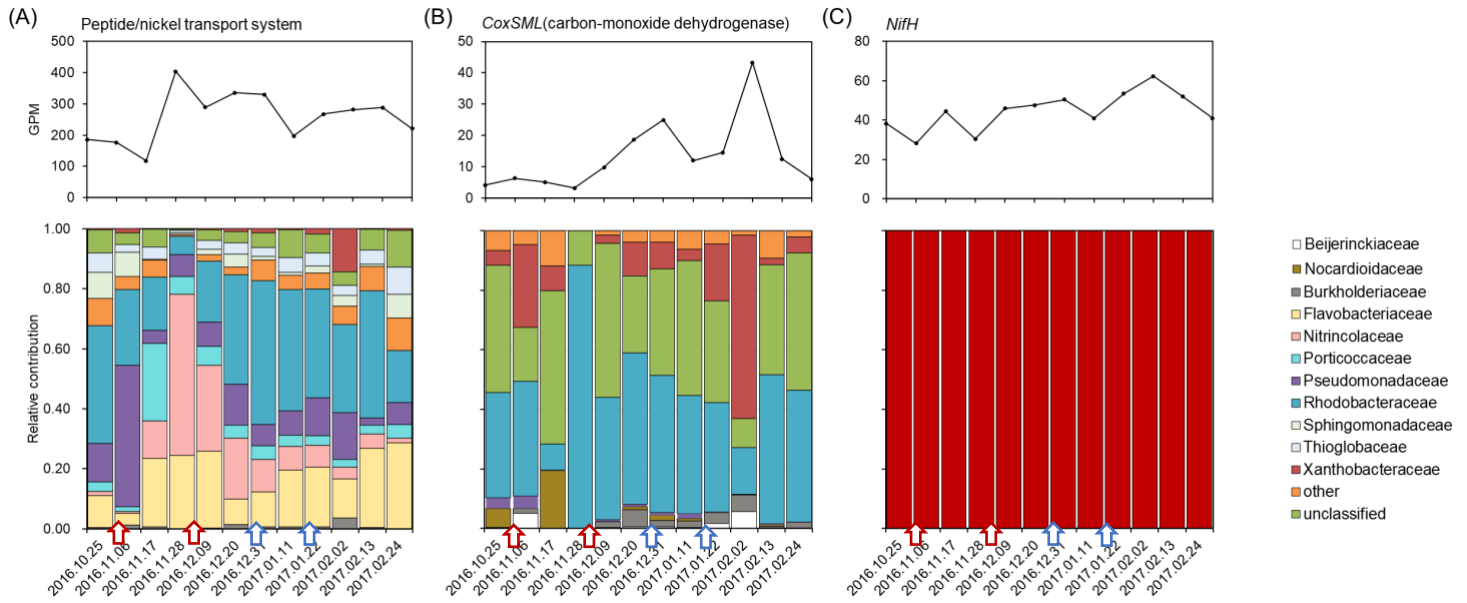


**Figure S6** Temporal changes of normalized gene abundance (GPM) and relative contribution of prokaryotic groups to peptide/nickel transport system (*ddp*, PE.P, PE.P1, PE.S) (A), carbon monoxide dehydrogenase (*coxSML*) (B) and nitrogen fixation gene (*nifH*) (C). Prokaryotic groups are based on the family level. Red arrows indicate the first spring phytoplankton bloom, and blue arrows indicate the second summer phytoplankton bloom.

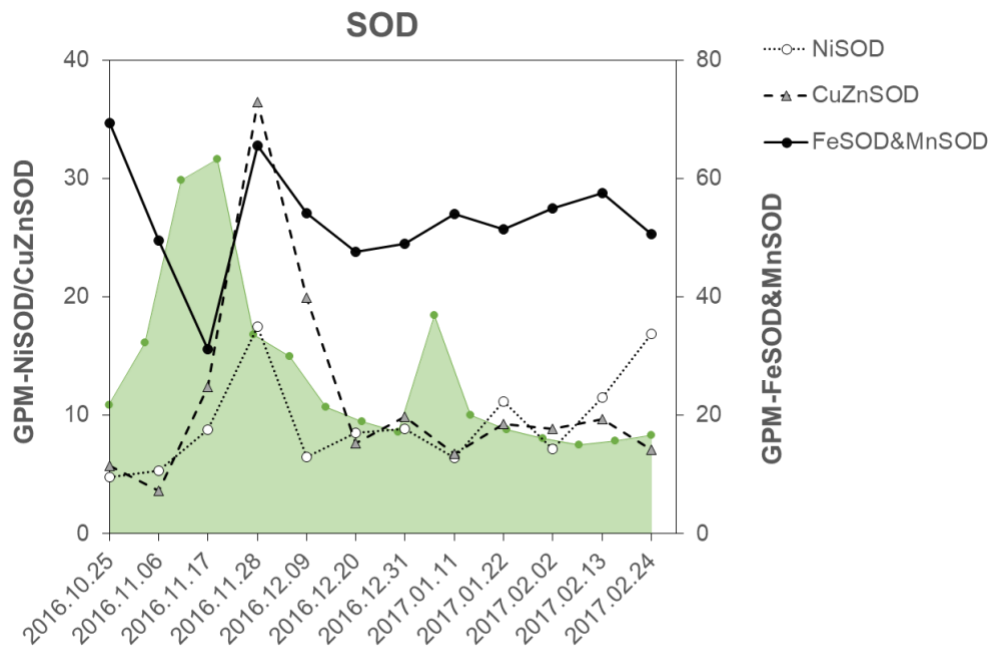


**Figure S7** Temporal changes of Chlorophyll a (green shaded area) and abundance of genes for different types of superoxide dismutases (SODs). Normalized gene abundances are given in genes per kilobase million (GPM).

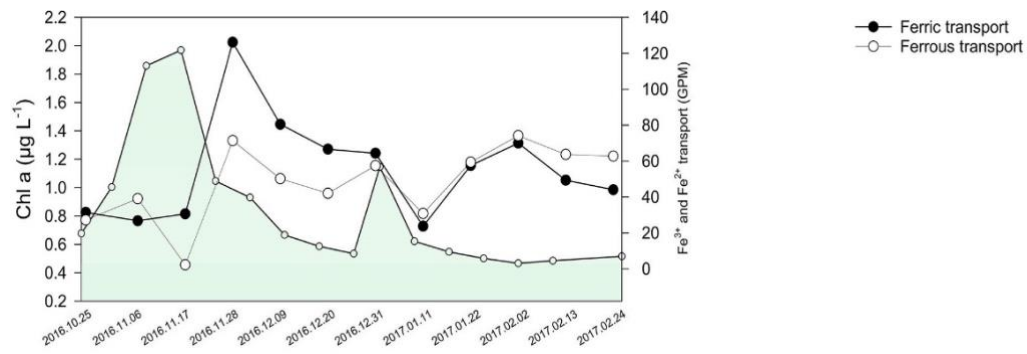


**Figure S8** Temporal changes of Chlorophyll *a* (green shaded area) and abundance of genes for  $\text{Fe}^{3+}$  and  $\text{Fe}^{2+}$  transporters. Normalized gene abundances are given in genes per kilobase million (GPM). Data are from Zhang *et al.* (2023).

## Reference

- Blain, S., Rembauville, M., Crispi, O., & Obernosterer, I. (2021). Synchronized autonomous sampling reveals coupled pulses of biomass and export of morphologically different diatoms in the Southern Ocean. *Limnology and Oceanography*, **66**(3), 753-764.
- Zhang, R., Debeljak, P., Blain, S., & Obernosterer, I. (2023). Seasonal shifts in Fe-acquisition strategies in Southern Ocean microbial communities revealed by metagenomics and autonomous sampling. *Environmental Microbiology*, **25**(10), 1816-1829.